

Comparison of the Effects of Daptomycin on Bacterial and Model Membranes

Ming-Tao Lee,^{†,‡} Pei-Yin Yang,[§] Nicholas E. Charron,[§] Meng-Hsuan Hsieh,^{||} Yu-Yung Chang,[†] and Huey W. Huang^{*,§,ⓑ}

[†]National Synchrotron Radiation Research Center, Hsinchu, Taiwan 300

[‡]Department of Physics, National Central University, Jhongli, Taiwan 320

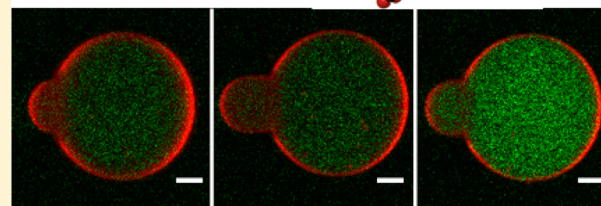
[§]Department of Physics and Astronomy, Rice University, Houston, Texas 77005, United States

^{||}Institute of Biotechnology, National Taiwan University, Taipei, Taiwan 10617

Supporting Information

ABSTRACT: Daptomycin is a phosphatidylglycerol specific, calcium-dependent membrane-active antibiotic that has been approved for the treatment of Gram-positive infections. A recent *Bacillus subtilis* study found that daptomycin clustered into fluid lipid domains of bacterial membranes and the membrane binding was correlated with dislocation of peripheral membrane proteins and depolarization of membrane potential. In particular, the study disproved the existence of daptomycin ion channels. Our purpose here is to study how daptomycin interacts with lipid bilayers to understand the observed phenomena on bacterial membranes. We performed new types of experiments using aspirated giant vesicles with an ion leakage indicator, making comparisons between daptomycin and ionomycin, performing vesicle–vesicle transfers, and measuring daptomycin binding to fluid phase versus gel phase bilayers and bilayers including cholesterol. Our findings are entirely consistent with the observations for bacterial membranes. In addition, daptomycin is found to cause ion leakage through the membrane only if its concentration in the membrane is over a certain threshold. The ion leakage caused by daptomycin is transient. It occurs only when daptomycin binds the membrane for the first time; afterward, they cease to induce ion leakage. The ion leakage effect of daptomycin cannot be transferred from one membrane to another. The level of membrane binding of daptomycin is reduced in the gel phase versus the fluid phase. Cholesterol also weakens the membrane binding of daptomycin. The combination of membrane concentration threshold and differential binding is significant. This could be a reason why daptomycin discriminates between eukaryotic and prokaryotic cell membranes.

Daptomycin expands the membrane area and causes ion leakage.



Daptomycin is a Food and Drug Administration-approved calcium-dependent antibiotic that specifically targets bacterial membranes, particularly that of Gram-positive bacteria.¹ Accumulated evidence so far consistently supports the role of the bacterial membranes being the central target for the action of daptomycin.^{1–12} Indeed, the mutations that alter susceptibility to daptomycin appear to directly affect the membrane lipid composition.^{8–12} In two examples, both the decrease in the level of phosphatidylglycerol (PG) synthesis and the increase in the level of conversion of PG to lysylphosphatidylglycerol found in the resistant mutants of *Staphylococcus aureus*¹³ and *Bacillus subtilis*¹⁴ led to reduced daptomycin activity. Electron microscopy showed that daptomycin does not cause cell lysis,^{7,15} nor does it cause leakage of molecules other than ions.^{5,7}

For years, the mode of action of daptomycin has been assumed to be leakage of potassium ions that leads to the loss of membrane potential and cell death.^{1–12,16} In lipid vesicle experiments, daptomycin causes ion leakage only when the

vesicles contain PG and in the presence of calcium ions,^{6,17} exactly the same condition found to be necessary for daptomycin to be effective against bacteria. However, recently Müller et al.¹⁸ performed an *in vivo* study on *B. subtilis* membranes using a combination of proteomics, ionomics, and fluorescence microscopy assays. They found evidence contradicting two previous hypotheses concerning the daptomycin mechanism; i.e., daptomycin forms ion channels in bacterial membranes,^{1,16,19,20} or daptomycin causes membrane curvature changes.^{21,22} Instead, they found that daptomycin selectively clusters to fluid membrane domains, dislocates several peripheral membrane proteins, and consequently triggers cell envelope stress. They also found daptomycin inducing depolarization of the membrane potential, which also

Received: August 5, 2018

Revised: August 26, 2018

Published: August 28, 2018

contributed to the delocalization of peripheral membrane proteins.¹⁸

Clearly, basic studies of daptomycin's interaction with lipid bilayers are useful for understanding the causes of the phenomena observed in the bacterial membranes. Müller et al.¹⁸ proposed a working model largely based on molecular interactions promoted by previous model membrane studies, but so far, there has been little information about how daptomycin structurally interacts with lipid bilayers and how daptomycin perturbs lipid bilayer properties. If daptomycin does not form ion channels, what is the nature of this ion leakage? Müller et al.¹⁸ suggested that clustering to fluid lipids by daptomycin likely causes hydrophobic mismatches between fluid and more rigid membrane domains that can facilitate proton leakage and explain the membrane depolarization. This idea can be tested by model membrane studies.

Here we report several new experiments investigating the interaction of daptomycin with lipid bilayers composed of 1,2-dioleoyl-*sn*-glycero-3-phosphocholine (DOPC) and 1,2-dioleoyl-*sn*-glycero-3-phospho(1'-*rac*-glycerol) (DOPG) or 1,2-dioleoyl-*sn*-glycero-3-phosphoethanolamine (DOPE) and DOPG, including (1) measurement of daptomycin-induced membrane area change and correlated ion leakage into micropipet-aspirated giant unilamellar vesicles (GUVs), (2) a test of the existence of ion channels by leakage of calcium ions into large unilamellar vesicles (LUVs), (3) a test of vesicle-vesicle transferability of daptomycin channels, and (4) the effects of bilayer fluidity on the interaction with daptomycin. All of our results are consistent with the observations by Müller et al.¹⁸ on bacterial membranes, including the absence of daptomycin ion channels. We observed a clear pattern of insertion of daptomycin into the lipid bilayers of GUVs. Ion leakage across the membrane occurs as the inserted daptomycin concentration reaches a certain threshold in the membrane. We also found that ion leakage occurs only transiently. Daptomycin indeed preferentially binds to fluid membranes, but it is unlikely that ion leakage is through the boundaries of membrane domains.

Leakage of potassium ions from *Staphylococcus aureus* induced by daptomycin (and independently by valinomycin) was first demonstrated by Silverman et al.¹ Zhang et al.¹⁷ compared the permeabilities to various ions through 1,2-dimyristoyl-*sn*-glycero-3-phosphocholine (DMPC)/1,2-dimyristoyl-*sn*-glycero-3-phospho(1'-*rac*-glycerol) (DMPG) bilayers, including PG dependence. Recently, Taylor et al.²³ published results suggesting that daptomycin induces ion permeability only through the DMPC/DMPG bilayer but not through DOPC/DOPG or phosphatidylcholine (POPC)/1-palmitoyl-2-oleoyl-*sn*-glycero-3-phosphoglycerol (POPG) bilayers. However, the same experimental method also showed no leakage of K⁺ by valinomycin. Because valinomycin is a typical control for a K⁺ leakage experiment (e.g., ref 1), the null result of valinomycin poses a question about this latest result. Our ion leakage experiments are designed to test specific features of interactions of daptomycin with membranes. The previous ion leakage experiments did not address the issues discussed in this paper.

MATERIALS AND METHODS

Materials. Daptomycin was purchased from Selleckchem (Munich, Germany; high-performance liquid chromatography purity of 99.81%). DOPC, DOPG, DOPE, DMPC, DMPG, and 1,2-dioleoyl-*sn*-glycero-3-phosphoethanolamine-*N*-liss-

amine rhodamine B sulfonyl (Rh-DOPE) were purchased from Avanti Polar Lipids (Alabaster, AL). Calcium indicator Fluo-4 was purchased from Life technologies (Grand Island, NY). Gramicidin, valinomycin, ionomycin, calcium chloride (>98.0%), and other reagents, all of the highest available purity, were purchased from Sigma-Aldrich (St. Louis, MO).

Giant Unilamellar Vesicle (GUV) Experiment. GUV experiments were performed in a setup described by Sun et al.²⁴ GUVs of a chosen lipid composition were produced by the electroformation method²⁵ in a solution containing 199 mM sucrose for the purpose of controlling the osmolality and 1 mM Tris at pH 7. The solution also contained 40 μ M calcium sensitive fluorescent dye Fluo-4²⁶ for the ion leak-in experiment. Ten microliters of a GUV suspension was injected into a control chamber that contained \sim 190 mM glucose and 10 mM Tris at pH 7. Sucrose is inside and glucose outside so that the GUVs sink to the bottom for the ease of micropipet aspiration. The osmolality of each solution used in the experiment was measured by a Wescor model 5520 vapor pressure osmometer (Wescor, Logan, UT) and was made the same as the osmolality of the solution inside the vesicles so that the vesicles were kept in equi-osmolality balance. A selected vesicle (diameter of 20–50 μ m) was aspirated at a low constant negative pressure (which created a membrane tension of 0.5–1 dyn/cm) by a micropipet connected to a pressure control system. [Before the experiment, micropipets (with inner diameters of 9–13 μ m) and the chamber walls were coated with 1% bovine serum albumin to dissipate the charge on the glass surface²⁷ and then washed extensively with Milli-Q deionized water.] The pressure control system was similar to the setup described by Kuchnir Fygenon et al.²⁸ The negative pressure was produced by connecting the micropipet to a syringe and was referenced to atmospheric pressure by a water-filled U tube. The pressure was measured by an MKS (Andover, MA) Baratron 223 pressure transducer with an MKS 660 digital readout.

To observe the effect of daptomycin on GUVs, the aspirated vesicle was transferred to an observation chamber that contained the control solution plus daptomycin and calcium ions. The observation chamber was set side by side with the control chamber, separated by \sim 0.5 cm. A transfer pipet (with an inner diameter of 0.75 mm) filled with the control solution was inserted into the control chamber through the observation chamber from the opposite side of the aspiration micropipet (details in ref 29). The aspiration pipet and the transfer pipet were each held by a model MM-188 motor-driven micro-manipulator (Narishige, East Meadow, NY). The vesicle transfer was accomplished by inserting the aspirated vesicle \sim 0.7 mm into the transfer pipet in the control chamber. When the microscope stage was moved, the observation chamber was translated to cover the position of the aspirated vesicle. Then the transfer pipet was moved away, so that the vesicle was now exposed to the observation chamber solution containing daptomycin (marked as $t = 0$). The solution in the observation chamber also had the same osmolality as the solution inside the GUV initially. However, in time water evaporation increased the osmolality of the solution in the chamber,^{28,29} which had a weak effect on the measurement of the increase in the membrane area (see below). For this reason, a transfer experiment is best limited to \sim 5 min.^{29,30}

In response to peptide binding, a GUV can change its membrane area A at constant volume V . The aspirated protrusion inside the micropipet serves as an amplifier for the

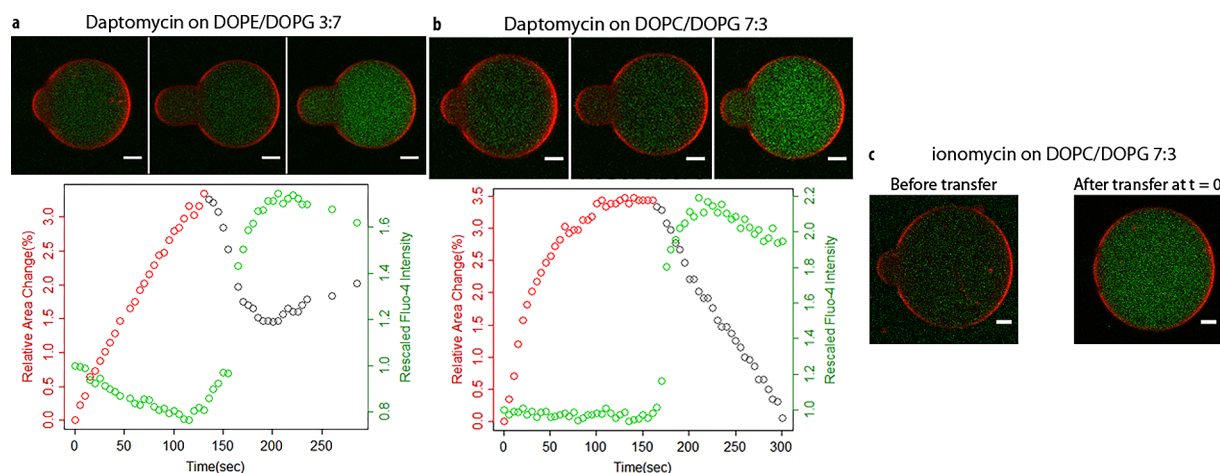


Figure 1. GUV transfer experiments. The solution inside the GUVs is the same: 199 mM sucrose, 1 mM Tris-HCl (pH 7.0), and 40 μ M Fluo-4. The common solution in the observation chamber consists of 187 mM glucose, 10 mM Tris-HCl (pH 7.4), and 1 mM CaCl_2 . (a) DOPE/DOPG (3:7) GUV transferred to a solution containing 0.3 μ M daptomycin. (b) DOPC/DOPG (7:3) GUV transferred to 1 μ M daptomycin. (c) DOPC/DOPG (7:3) GUV transferred to 0.2 μ M ionomycin. From the GUV protrusion, the relative membrane area change was calculated (red data). The same protrusion–area relation was used to indicate the change in protrusion length after the leakage occurred (gray data) (see [Materials and Methods](#)). Green data are the relative change in the fluorescence intensity of Fluo-4 inside the GUV. Confocal images were recorded for \sim 5 min. In panels a and b, the three GUV images from left to right are after the transfer at $t = 0$, near the maximum area expansion, and after the fluorescence intensity increase. The scale bar is 5 μ m [movies for panels a and b in the Supporting Information ([Movies 1a](#) and [1b](#), respectively)]. In panel c, the images are those before the transfer and immediately after the transfer. The first image after the transfer shows that, at $t = 0$, the protrusion length already shrank to zero and the fluorescence intensity already increased, indicating that ionomycin leaked ions as soon as it bound to the membrane.

measurement of such changes under a constant tension.³¹ From the microscopic images, L_p (the length of the protrusion), R_p (the radius of the micropipet), and R_v (the radius of the spherical part of the GUV) are carefully measured. Then it is straightforward to show $\Delta A = 2\pi R_p \Delta L_p + 8\pi R_v \Delta R_v$, and $\Delta V = \pi R_p^2 \Delta L_p + 4\pi R_v^2 \Delta R_v$.³¹ In general, the changes in the spherical radius ΔR_v are too small to be measured accurately. However, if there is no molecular (other than H_2O) leakage, and the inside and outside of the GUV are in iso-osmolality, there should be no change in volume. Under the condition where $\Delta V = 0$, ΔA is directly proportional to ΔL_p : $\Delta A = 2\pi R_p (1 - R_p/R_v) \Delta L_p$. In [Figure 1](#), this formula was used to translate ΔL_p to ΔA . This relation gives important information about the membrane area change ($\Delta A/A$) due to daptomycin binding before ion leakage occurs. After ion leakage occurs, this relation is no longer valid because ΔV is no longer zero, but in [Figure 1](#), for the sake of the continuation of data, we continued to use this formula for $\Delta A/A$ during ion leakage, only to show the changes in L_p . The video image of the experiment was recorded by a Nikon NS-5 MC camera.

Control experiments show that water evaporation in the observation chamber produces a slow background increase in protrusion length. This is because the osmolality imbalance causes water efflux resulting in a small decrease in the GUV volume. A ΔV of <0 and a ΔA of 0 produce a ΔL_p of >0 . This causes a small error in the estimate of the membrane area increase due to daptomycin binding.

Unilamellar Vesicles for the Ion Leakage Experiment (LUV) and for Circular Dichroism (CD) Measurement (SUV). Submicrometer-sized unilamellar liposomal vesicle suspensions with a low polydispersity were prepared as follows. Lipids with a chosen composition were dissolved in chloroform and dried under a gentle nitrogen flow and, subsequently, under vacuum for several hours to remove residual solvent. A 10 mM Tris buffer (pH 7.4) was added to the lipid dry film. The dispersion was shaken for 10 min and placed in an

ultrasonic bath for 50 min. The suspension was frozen and thawed between liquid nitrogen and 40 $^\circ\text{C}$ water six times. To prepare for large unilamellar vesicles (LUVs), the suspension was extruded 20 times through polycarbonate filters with a pore size of 100 nm at 40 $^\circ\text{C}$. The diameter of the vesicles was estimated by dynamic light scattering (DLS) (Malvern Zetasizer Nano S90) to be 80 ± 5 nm. To prepare for small unilamellar vesicles (SUVs), the suspension was sonified for 40 min until the solution looked transparent. The diameter of the SUVs was determined by DLS to be 40 ± 2 nm.

Calcium Ion Leak-In Experiment. DOPC/DOPG (7:3) LUVs were produced in a 10 mM Tris buffer (pH 7.4) containing 10 μ M Fluo-4²⁶ to give an LUV suspension of 100 or 200 μ M in lipid. LUVs encapsulating 10 μ M Fluo-4 were separated from the free dye in solution by running the suspension through a 1.5 mL PD-10 column containing Sephadex G-25 Medium twice with the Tris buffer as the eluent.

The fluorescence intensity of Fluo-4 was monitored, using a Jasco (Tokyo, Japan) FP-6000 spectrofluorometer, with an excitation wavelength of 494 nm and an emission wavelength of 518 nm at 25 $^\circ\text{C}$. The background intensity was first recorded for 120 s, and then a solution of CaCl_2 was added and the mixture observed for an additional 120 s before daptomycin or ionomycin was added. The mixtures were stirred (with a magnetic stirrer) constantly during the measurement. The integrity of vesicles was monitored by DLS.

Potassium Ion Leak-Out Experiment. DOPC/DOPG (7:3) LUVs were produced in a 10 mM Tris buffer (pH 7.4) containing 1 mM KCl to give an LUV suspension of 1 or 1.5 mM in lipid. Potassium ion-containing LUVs were separated from the free potassium ions in solution by running the suspension through a 1.5 mL PD-10 column containing Sephadex G-25 Medium twice with the Tris buffer as the eluent. The electric potential proportional to the logarithm of the potassium ion concentration in solution³² was monitored

using a World Precision Instruments (Sarasota, FL) KWIKPOT-2 potassium ion selective electrode connected to a HACH (Loveland, CO) sensION PH meter at 25 °C (see the [Supporting Information](#)). The potential reading was normalized to the maximum value when Triton X-100 was introduced to lyse the LUVs. Note that daptomycin in Tris buffer gave rise to a small potential reading (see [Results and Discussion](#)).

Two types of experiments were performed. (1) The background K^+ potential of the LUV suspension was first recorded for 600 s, and then a solution of daptomycin was added and observed for an additional 600 s before $CaCl_2$ was added. (2) In another K^+ leakage experiment, instead of introducing molecular agents into the LUV suspension, we introduced LUVs premixed with daptomycin, valinomycin, or gramicidin. The LUVs premixed with daptomycin, valinomycin, or gramicidin were produced the same way as normal LUVs, except that the membrane-active molecules were mixed with lipid in chloroform during LUV production. The following molar ratios were used: 1:80 gramicidin:lipid, 1:80 valinomycin:lipid, and 1:10:5 daptomycin:lipid:Ca. Ca ions were added to the daptomycin/LUV suspension. In all experiments, the mixtures were stirred (with a magnetic stirrer) constantly during the measurement.

Circular Dichroism. CD spectra were recorded in a Jasco J-815 spectropolarimeter with 4 μM daptomycin in a 10 mm cuvette. All samples were in 10 mM Tris buffer (pH 7.4). Lipid mixtures were in the form of SUVs (instead of LUVs to avoid light scattering). Samples were thoroughly mixed before measurement. Each CD spectrum was measured from 280 to 200 nm, and each sample was measured twice to make sure there was no change in the spectrum with time. We found that some mixtures took up to 20 min to reach equilibrium after mixing. For details, see ref 33.

RESULTS AND DISCUSSION

The lipid compositions of Gram-positive bacteria are dominated by PE and PG.³⁴ However, the physical states of PE and PG mixtures at room temperature are not planar bilayers, unless PE is a minority, because the spontaneous curvature of PE is strongly negative whereas the curvature of the outer leaflet of a vesicle is positive. Hence, we chose 3:7 DOPE/DOPG mixtures as a model membrane. As we will show below, the responses of 3:7 DOPE/DOPG GUVs and 7:3 DOPC/DOPG GUVs to daptomycin are similar. The molecular states of daptomycin bound to membranes are also the same in PE/PG and PC/PG GUVs, as measured by CD ([Figure S1](#)). For the sake of the ease of the experiment (e.g., the production of GUVs from PC and PG is better than from PE and PG, and we are also concerned about the quality of small vesicles made of PE and PG, which is difficult to detect), we have chosen to use PC/PG mixtures for the majority of experiments. For the studies investigating the interaction of daptomycin with fluid phase versus rigid phases, we used DOPC/DOPG/cholesterol mixtures and DMPC/DMPG mixtures. The DMPC/DMPG mixture was chosen because of its gel phase property below room temperature.³⁵

Earlier vesicle experiments^{36,37} with daptomycin and calcium ions found vesicle aggregation or fusion occurred at high concentrations of daptomycin and Ca^{2+} . In fact, both fusion and aggregation of vesicles can occur because of the presence of Ca^{2+} alone, and the occurrence of fusion also depends on the vesicle concentration.³⁸ Therefore, a careful choice of lipid,

daptomycin, and Ca concentrations is essential. We found that constant stirring of the suspension helped to homogenize the mixture (shorten the equilibration time³³) and perhaps prevent clustering of vesicles. We have examined the vesicles by DLS under the conditions of our ion leakage experiments ([Figure S2](#)) to make sure that our results are not affected by vesicle aggregation or fusion.

Response of Aspirated GUVs to Daptomycin and Ionomycin. The 3:7 DOPE/DOPG and 7:3 DOPC/DOPG GUVs were used to perform the transfer experiment to a chamber containing daptomycin and calcium ions. All GUVs included 1% Rh-DOPE to make the contour of the GUV clear under fluorescence inspection. The solution inside the GUVs is the same: 199 mM sucrose, 1 mM Tris-HCl (pH 7.0), and 40 μM Fluo-4. The common solution in the observation chamber consists of 187 mM glucose, 10 mM Tris-HCl (pH 7.4), and 1 mM $CaCl_2$. The reason for including sucrose and glucose is explained in [Materials and Methods](#). We chose a calcium concentration of 1 mM, which is close to the concentration in human serum.³ Daptomycin concentrations in the range of the minimum inhibitory concentrations (MICs), which are in low micromoles per liter, were chosen.^{3,39} Panels a–c of [Figure 1](#) show the results of an aspirated 3:7 DOPE/DOPG GUV transferred to a solution containing 0.3 μM daptomycin, a 7:3 DOPC/DOPG GUV transferred to 1 μM daptomycin, and a 7:3 DOPC/DOPG GUV transferred to 0.2 μM ionomycin, respectively. The concentrations of daptomycin and ionomycin were adjusted so that the ion leakage occurred within 5 min. The response of the 3:7 PE/PG mixture to 0.3 μM daptomycin is similar to the response of the 7:3 PC/PG mixture to 1 μM daptomycin. The difference in daptomycin concentration could be due to the difference in the PG ratio; i.e., a higher PG ratio (3:7 PE/PG) requires a lower daptomycin concentration (0.3 μM). As mentioned in [Materials and Methods](#), water evaporation slowly increased the osmolality of the chamber solution relative to the GUV interior. The resulting water efflux would increase the GUV protrusion.²⁹ Control experiments ([Figure S3](#)) show that the background increase in the protrusion length is much smaller than the changes caused by daptomycin within 5 min. Also shown in [Figure S3](#) is the effect of photobleaching of calcium-activated Fluo-4 fluorescence.

At the moment of transfer ($t = 0$), the inside and outside of the GUVs had the same osmolality. The subsequent increase in the GUV membrane area in the absence of ion leakage indicates the binding of daptomycin to the lipid bilayer. It is important to note that the membrane binding of daptomycin continued for a period of time without causing ion leakage. Once calcium ions leak-in had occurred, as indicated by the increase in the fluorescence intensity of Fluo-4 inside the GUV, the protrusion length began to decrease. This is because the inside osmolality increased due to the influx of calcium ions that in turn caused water influx and the GUV volume increase. The relatively rapid volume increase with an approximately constant membrane area will cause the protrusion length decrease.²⁹ (In [Figure 1](#), the protrusion length decrease is expressed as the membrane area decrease as explained in [Materials and Methods](#).) The responses seen in panels a and b of [Figure 1](#) are to be compared with the response to ionomycin ([Figure 1c](#)). Ionomycin is a well-known ionophore or ion carrier that is capable of transferring calcium ions between two sides of the membrane.⁴⁰ In this case, as soon as the GUV was transferred, the first ($t = 0$) image

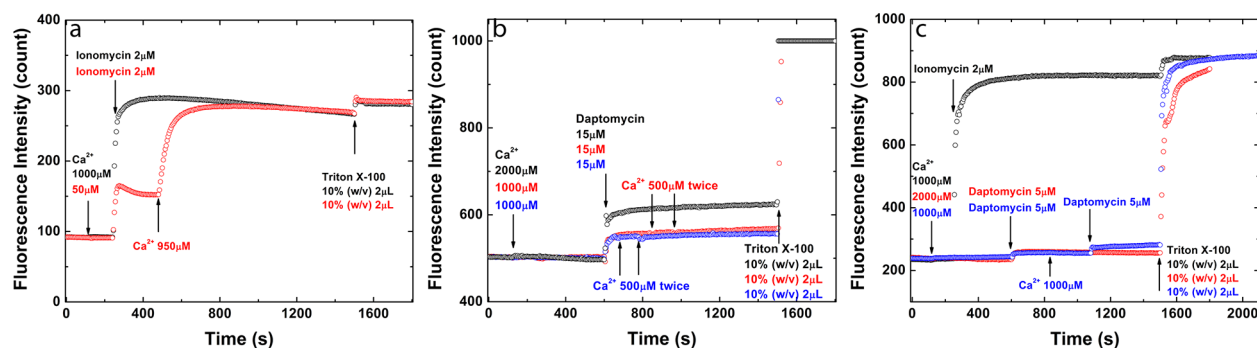


Figure 2. Calcium ion leak-in experiment. The samples were (a and b) 200 μM or (c) 100 μM DOPC/DOPG (7:3) LUVs encapsulating 10 μM Fluo-4. The subsequent actions are indicated within the figure, while the fluorescence intensity of Fluo-4 was continually monitored. Finally, 2 μL of a 10% (w/v) Triton X-100 solution was added at 1500 s to break up the vesicles. (Note that the levels of fluorescence intensity amplification were different for panels a–c.) (a) Effect of ionomycin. For the black trace, first 1000 μM Ca^{2+} was added followed by addition of 2 μM ionomycin. For the red trace, 50 μM Ca^{2+} , then 2 μM ionomycin, and then 950 μM Ca^{2+} were added. (b) Effect of daptomycin. For the black trace, 2000 μM Ca^{2+} and then 15 μM daptomycin were added. For the red trace, 1000 μM Ca^{2+} , then 15 μM daptomycin, and then 500 μM Ca^{2+} (twice) were added. The blue is a repeat of the red trace. (c) Comparison of daptomycin with ionomycin. For the black trace, 1000 μM Ca^{2+} and then 2 μM ionomycin were added. For the red trace, 2000 μM Ca^{2+} and then 5 μM daptomycin were added. For the blue trace, 1000 μM Ca^{2+} , then 5 μM daptomycin, then 1000 μM Ca^{2+} , and then 5 μM daptomycin were added.

showed that the Fluo-4 fluorescence intensity had already increased and the protrusion length had already decreased to a minimum. Ion leakage occurred as soon as the GUV was exposed to ionomycin.

The response of DOPC/DOPG GUVs to daptomycin has been investigated extensively without an ion leakage indicator in a previous paper.⁴¹ The responses observed in panels a and b of Figure 1 are the same as the previous observation. In the prior study,⁴¹ we discovered the lipid extraction effect that was correlated with the GUV protrusion length decrease. For this reason, lipid extraction was thought to be the reason for the membrane area decrease (at that time, we did not know it was correlated with ion leakage). We now believe that this is an incorrect explanation even if lipid extraction contributes to the membrane area decrease. We believe that the correct explanation for the protrusion length decrease is the ion leak-in that increases the osmolality of the GUV interior as explained above. It is instructive to compare Movies 1a and 1b with the response of GUV to melittin³⁰ (reproduced in the Supporting Information for the sake of convenience). Both daptomycin and melittin initially bind to the membrane and expand the membrane area with no change in the GUV interior. Then when the bound peptide:lipid ratio reaches a threshold, leakage occurs. In the case of melittin, pores were formed in the GUV membrane that leaked the dye molecules initially encapsulated inside.³⁰ Here daptomycin causes leak-in of calcium ions but no leak-out of Fluo-4 molecules. In our previous study, we showed that daptomycin did not cause leak-out of encapsulated dye molecules of Texas Red sulfonyle chloride.⁴¹

The confocal images shown in Figure 1 and and movies in the Supporting Information did not show the lipid extraction effect that is clearly seen in epifluorescent images in ref 41 and Figure 6. Interestingly, while the lipid extraction was seen in every run with DOPC/DOPG GUVs, it was absent for the DOPE/DOPG GUVs. We do not know if lipid extraction was absent in the case of DOPE/DOPG GUVs or if the lipid extractions were too small to be visible with a microscope. For example, the peptide/lipid aggregates induced by penetratin are visible in charged lipids but not in neutral lipids, even

though there is evidence from X-ray diffraction that penetratin/lipid aggregates occurred in both cases.^{42,43}

Recently, Kreutzberger et al.⁴⁴ observed co-aggregation of daptomycin and fluorescent lipid TopFluor-PS in POPC/POPG bilayers. In their confocal images, the aggregates look similar to the peptide/lipid aggregates seen in the lipid extraction phenomena.⁴¹ However, the authors⁴⁴ believed that the aggregates represented clustering domains of daptomycin with POPG in the membrane.

Transient Nature of Ca^{2+} Leak-In Induced by Daptomycin. The Ca^{2+} leak-in experiments were performed using 0.1 μm large unilamellar vesicles (LUVs) encapsulating calcium indicator Fluo-4.²⁶ The Fluo-4 fluorescence intensity of the LUV suspension would increase if Ca^{2+} in the solution leaked across the membrane into the LUVs, as seen in the GUV interior described in Figure 1. We compared the effect of daptomycin with that of ionomycin.

In all the Ca^{2+} leak-in experiments, time zero is the beginning of the fluorescence intensity measurement of an LUV suspension. In Figure 2a, we first added 1 mM Ca^{2+} to the LUV suspension, followed by 2 μM ionomycin. The leakage of Ca^{2+} across the LUV membranes caused an increase in fluorescence intensity from 90 to ~ 290 counts. In the next run, we introduced 50 μM Ca^{2+} followed by 2 μM ionomycin. As expected, the fluorescence intensity increase was smaller than in the previous run, but then at ~ 500 s, we added another calcium solution to make the total external Ca^{2+} concentration 1 mM. This further calcium ion influx increased the fluorescence intensity to the level reached by the first run. In both runs, 2 μL of a 10% (w/v) Triton X-100 solution was added at 1500 s to break up the vesicles. This experiment showed that ionomycin is functioning in the membrane as an ion carrier, exactly as expected.

The effect of daptomycin is much weaker than that of ionomycin. Thus, in Figure 2b, the fluorescence intensity was amplified ~ 5 -fold compared with that in Figure 2a (note the difference in the background intensities). We started daptomycin experiments first with 2 mM Ca^{2+} followed by 15 μM daptomycin (Figure 2b). In the next two runs, we added 1 mM Ca^{2+} followed by 15 μM daptomycin. Afterward, at various times, calcium solutions were added first to a total

concentration of 1.5 mM and subsequently to a total Ca^{2+} concentration of 2 mM. Contrary to the case of ionomycin, no fluorescence intensity increase occurred when additional Ca^{2+} was added. Again at 1500 s, Triton X-100 was added to break up the vesicles. (Note that in this setting of fluorescence intensity, the addition of Triton X-100 oversaturated the maximum intensity scale of the instrument.) This experiment showed that daptomycin induced ion leakage shortly after being introduced into the LUV suspension, but it ceased to cause ion leakage afterward, in contrast to ionomycin, which transferred the ions any time additional extravesicular Ca^{2+} was added.

In Figure 2c, we adjusted the fluorescence intensity amplification setting so that the effects of both ionomycin and daptomycin could be compared. For daptomycin, we had two runs: one with 1 mM Ca^{2+} and another with 2 mM Ca^{2+} , both followed by 5 μM daptomycin. As in Figure 2b, the suspension with an initial Ca^{2+} concentration of 1 mM was later added to 2 mM Ca^{2+} without any fluorescence increase being noticeable. However, when we subsequently added additional 5 μM daptomycin, additional ion leakage and a fluorescence increase occurred, consistent with the observation in Figure 2b that daptomycin caused ion leakage only immediately after it was introduced into the suspension. We have repeated all of these leakage experiments multiple times. The results were reproducible without exception. For a quantitative comparison of the leakage activities by daptomycin and ionomycin, we show that leakage with 15 μM daptomycin is comparable to the leakage with 0.01 μM ionomycin (Figure 3 and Figure S4). The ion leakage effect of

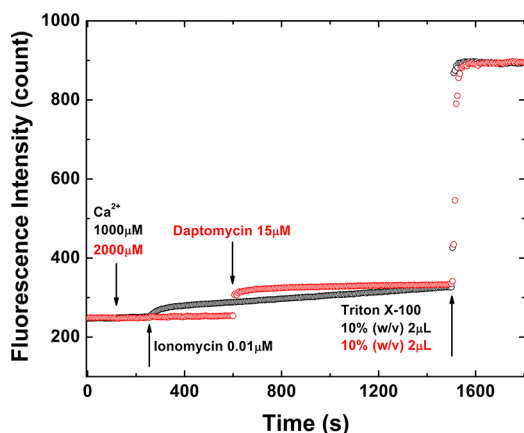


Figure 3. Quantitative comparison of the effects of daptomycin and ionomycin. All samples were 200 μM LUVs (of 7:3 DOPC/DOPG) encapsulating 10 μM Fluo-4. The effect of 15 μM daptomycin (with 2 mM Ca^{2+}) is comparable to the effect of 0.01 μM ionomycin (with 1 mM Ca^{2+}). The slow increase in ion leakage caused by 0.01 μM ionomycin is confirmed by the concentration dependence shown in Figure S4.

daptomycin is 1500 times weaker than that of ionomycin. Additionally, as a control, we show that daptomycin causes Ca^{2+} leak-in only in membranes containing PG (Figure S5).

Test of Vesicle–Vesicle Transferability of Daptomycin Channels by K^+ Leak-Out. In the control experiment for leakage of K^+ from LUVs (Figure 4a), the background K^+ potential (Figure S6) of the suspension of K^+ -encapsulating LUVs was first recorded for 600 s. Then a solution of daptomycin without Ca^{2+} was added to the suspension, and the

suspension observed for another 600 s. Note that daptomycin in a K^+ free solution gives rise to a potential reading (see Figure S7). This background was removed from Figure 4a, where time zero is when the daptomycin was added. We then added CaCl_2 to the LUV suspension that activated the reaction of daptomycin with the LUV membranes causing leakage of K^+ from the LUVs.

In the second K^+ experiment (Figure 4b), we made use of the known experimental fact of vesicle–vesicle exchange of molecules in a vesicle suspension.^{45–47} We prepared two sets of LUVs. In one set, we mixed gramicidin, valinomycin, or daptomycin separately in the lipid mixtures for the formation of gramicidin LUVs, valinomycin LUVs, or daptomycin-LUVs, respectively, in 1:80 gramicidin:lipid, 1:80 valinomycin:lipid, and 1:10:5 daptomycin:lipid:Ca molar ratios. In another set, we prepared K^+ -encapsulating LUVs. K^+ ions outside the LUVs were removed. Then each of the first set of LUVs was introduced into a suspension of K^+ -encapsulating LUVs, and the K^+ potential was recorded. The result is shown in Figure 4b. The ion channel gramicidin and ion carrier valinomycin were transferred to the K^+ -encapsulating LUVs and caused leakage of K^+ ; on the contrary, daptomycin did not cause leakage of K^+ .

Gel Phase versus Fluid Phase and the Effect of Cholesterol. It has recently been demonstrated³³ that the system consisting of three components, i.e., daptomycin, calcium ions, and PG-containing membranes, as a function of their concentrations, exhibits only two basis CD spectra. The state of monomeric daptomycin in the absence of one or two other components has a unique CD spectrum called the A state. This is the nonbinding state of daptomycin. Daptomycin with excessive calcium and PG has another distinct CD spectrum called the B state. This is the membrane-bound state of daptomycin. Under all other conditions, the CD of the system is a linear combination of A and B (Figure S1). Furthermore, we have established the stoichiometric daptomycin: Ca^{2+} :PG ratios in the B state to be 2:3:2, assuming only the PGs in the outer layer of vesicles are available for reaction.³³ (The ratios would be 2:3:4 if all PGs in the vesicles are available for reaction.³³)

In the gel phase experiment, 7:3 DMPC/DMPG SUVs were produced and kept at 20 °C in the gel phase.³⁵ First, daptomycin was added to a final concentration of 4 μM and measured for the A spectrum (Figure 5). Next, CaCl_2 was added to make a suspension of 4 μM daptomycin, 80 μM DMPC/DMPG, and 100 μM Ca^{2+} to measure the gel phase spectrum at 20 °C (Figure 5). The result was 35% A and 65% B. The sample was then warmed and measured at 24, 28, 32, and 36 °C. At each change in temperature (say, at $t = 0$ min), the CD measurement was taken at 10 min and again at 20 min. In each case, the CD change occurred within 10 min. The repeat measurement at 20 min showed no further change in CD. The spectrum gradually changed with temperature to 100% B. Subsequently, the CD was measured as the temperature was decreased to 20 °C. The CD remained constant at 100% B as the temperature was decreased. It is important to note that the daptomycin spectra A and B measured with DMPC and DMPG (Figure 5) or with DOPE and DOPG (Figure S1) are quite similar to the spectra measured with DOPC and DOPG³³ (Figure S1), implying that the bound state of daptomycin is relatively insensitive to the lipid species.

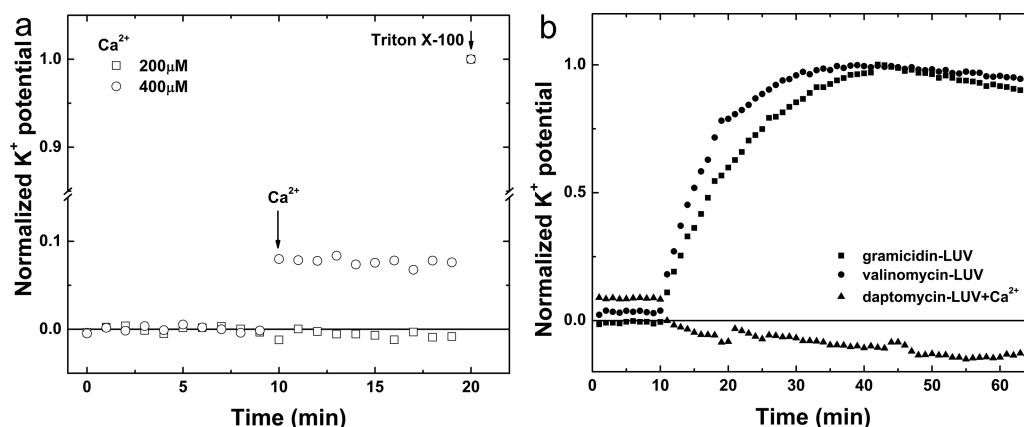


Figure 4. Potassium ion leakage experiments were performed with K^+ -encapsulating 1 mM DOPC/DOPG (7:3) LUVs. (a) Daptomycin alone in Tris buffer gave rise to a small potential reading (Figure S7). This background was removed from the leakage data. The leakage of K^+ from the LUVs caused by daptomycin was activated by the addition of Ca^{2+} . (b) Gramicidin, valinomycin, and daptomycin were each mixed into the DOPC/DOPG lipid mixture to form gramicidin LUVs, valinomycin LUVs, and daptomycin LUVs, respectively. ($CaCl_2$ was added to daptomycin LUVs.) These peptide LUVs were each separately added to a suspension of DOPC/DOPG LUVs encapsulating 1 mM KCl. Potassium ion leakage was seen in the case of gramicidin LUVs and valinomycin LUVs but not in the case of daptomycin LUVs.

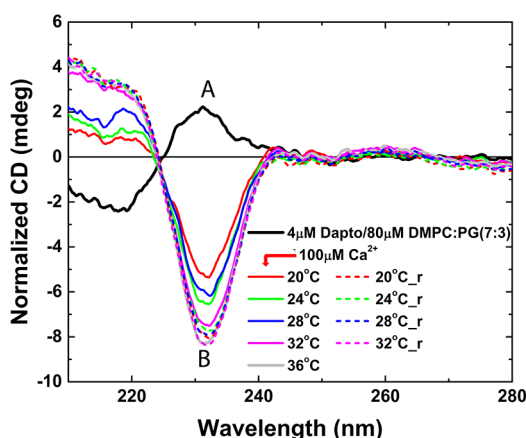


Figure 5. Binding of daptomycin to gel phase lipid bilayers. DMPC/DMPG (7:3) vesicles (at a lipid concentration of 80 μ M) were kept at 20 $^{\circ}$ C. First, 4 μ M daptomycin was added for the measurement of the A spectrum. Then 4 μ M daptomycin and 100 μ M $CaCl_2$ were added to measure the CD that showed 35% A and 65% B. Then the temperature was increased stepwise to 36 $^{\circ}$ C (solid color lines), as the percent of B increased to 100%. The CD was measured 10 and 20 min after each change in temperature. In each case, the change in CD occurred within 10 min. No further change in CD was found between the two measurements. The temperature was then decreased to 20 $^{\circ}$ C (dashed color lines). The spectrum did not change when the temperature was decreased.

It is clear that the initial gel phase exhibits resistance (or partial resistance) to daptomycin binding; only 65% of the total, available daptomycin molecules were bound. But once the bilayers were warmed to a sufficiently high temperature to become a fluid phase, the binding became 100%. The persistence of the 100% B state when the temperature was decreased to 20 $^{\circ}$ C has no obvious explanation. It is possible that the state of DMPC and DMPG with the bound daptomycin is no longer in the gel phase at 20 $^{\circ}$ C.

In the next experiment, we tested the effect of cholesterol on the daptomycin binding reaction (Figure 6). We performed the same transfer experiment as described in Figure 1b with aspirated DOPC/DOPG/cholesterol GUVs at ratios of 7:3:0, 6:3:1, and 4:3:3 to observe the cholesterol effect (note that the

daptomycin:PG ratio is the same in all cases). The addition of cholesterol has two effects. First, we found that the speed of GUV membrane area expansion decreased with the inclusion of cholesterol, implying a slowdown of the daptomycin binding reaction with the lipid bilayer. Second, the amount of lipid extraction also decreased with an increasing content of cholesterol. In fact, lipid extraction was not visible with 30% cholesterol added to the GUVs (Figure 6).

SUMMARY

Our experimental results with model membranes are consistent with the two major observations of bacterial membranes described by Müller et al.¹⁸

1. Daptomycin Binding Varies with the Fluidity of Lipid Bilayers. In the bacterial study, daptomycin was found to preferentially bind to fluid membrane domains. We found that the binding ratio of daptomycin to the fluid phase of the DMPC/DMPG mixture at 36 $^{\circ}$ C versus the gel phase at 20 $^{\circ}$ C is 100:65. Inclusion of cholesterol is known to have a condensing effect⁴⁸ that rigidifies or stiffens⁴⁹ the lipid bilayers. We found that the rate of binding of daptomycin to membrane is decreased in proportion to the content of cholesterol included in the lipid bilayer. This could be a protective factor for the eukaryotic cells against the attack of daptomycin, because sterols are present only in eukaryotic cell membranes.

2. Daptomycin Induces Ion Leakage but Does Not Form Ion Channels. Müller et al.¹⁸ found daptomycin capable of inducing depolarization of the membrane potential. They argue against the existence of daptomycin ion channels based on their findings that the effect of daptomycin is extremely weak compared with the effect of standard ion channels or ionophores such as gramicidin or valinomycin. Gramicidin is a well-characterized monovalent cationic ion channel.⁵⁰ Valinomycin⁵¹ is a well-characterized K^+ carrier similar to the Ca^{2+} carrier ionomycin.⁴⁰

Ion leakage caused by daptomycin for various species of ions has been demonstrated previously.^{1,17,23} Here we studied the nature of this ion leakage effect with three different experiments: calcium ion leak-in to GUVs (Figure 1), calcium ion leak-in to LUVs (Figure 2), and potassium ion leak-out from LUVs (Figure 4).

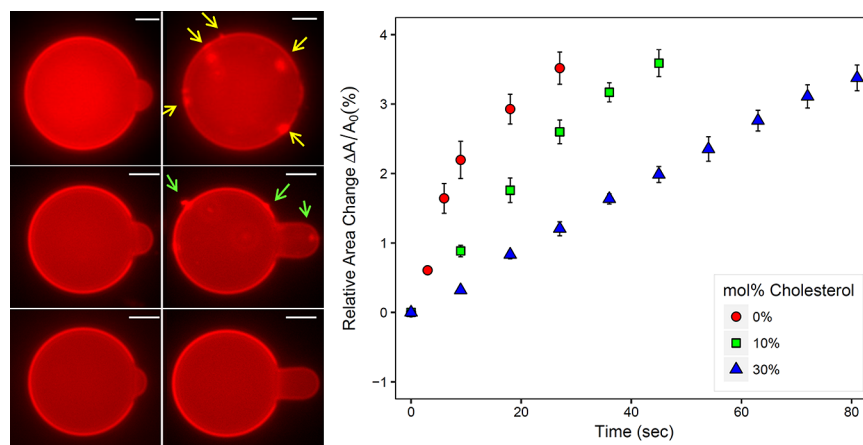


Figure 6. Effect of cholesterol on the daptomycin binding reaction. The same transfer experiment was performed as described in Figure 1b with DOPC/DOPG/cholesterol GUVs at ratios of 7:3:0, 6:3:1, and 4:3:3 in a solution containing 1 μM daptomycin and 1 mM CaCl_2 . The GUV area first increased and then decreased as shown in Figure 1b. Here, only the increases in membrane area are shown for comparison. Three rows of epifluorescent images are shown from top to bottom in order of increasing cholesterol content. At left are the images at $t = 0$. At right are images during the protrusion length decrease when the lipid extraction effect occurred. Arrows indicate daptomycin/lipid aggregates (lipid extraction);⁴¹ none was found for the GUV with 30% cholesterol. The right panel shows the rate of the initial area expansion of the GUVs. The rate decreases with an increase in cholesterol content. The mean and the standard deviation of the mean are obtained from multiple measurements. The scale bar is 10 μm .

First, we showed that the ion leakage effect of daptomycin is 3 orders of magnitude weaker than that of ionomycin (Figure 3), consistent with the finding of Müller et al. that daptomycin is a weak ion leaker.

In addition, we showed that daptomycin induces only transient ion leakage. In the LUV experiment (Figure 2), daptomycin causes ion leakage only when the molecules are introduced into the vesicle suspension for the first time. Afterward, they cease to induce ion leakage. This unique property of daptomycin is most clearly demonstrated via a comparison with ionomycin. Once ionomycin molecules enter a membrane and form ion carriers, these carriers transmit ions every time additional calcium ions are added to the solution. This is not the case for daptomycin. Daptomycin appears to cause transient ion leakage only at the initial contact with membranes in the presence of sufficient Ca^{2+} . After the transient effect, they have no further ion leakage effect, even if additional Ca^{2+} is added.

In the potassium ion leak-out experiments, we compared daptomycin with gramicidin ion channels and valinomycin ion carriers (Figure 4). We first mixed daptomycin, gramicidin, and valinomycin each into PC/PG lipid vesicles; these vesicles contained no K^+ ions. We then mixed each type of vesicle with K^+ -encapsulating vesicles that contained no daptomycin, gramicidin, or valinomycin. Our experiment showed that both gramicidin and valinomycin can be transferred from no- K^+ vesicles to K^+ -encapsulating vesicles and subsequently cause leakage of ions from the K^+ -encapsulating vesicles. This is consistent with the known experimental finding^{45–47,52} that there is a vesicle-vesicle exchange of molecules in a vesicle suspension. Thus, we expect daptomycin complexes to be transferred between vesicles. However, our results show that the transferred daptomycin did not cause ion leakage (Figure 4). Thus, if there are daptomycin complexes within lipid bilayers, they do not function as ion channels.

Perhaps the transient nature can explain why the overall ion leakage effect of daptomycin is weak as detected by Müller et al.¹⁸ and as measured in Figure 3. It can also explain the nontransferability as demonstrated in the experiment depicted

in Figure 4. Neither the idea of ion channels^{17,53–55} nor the idea of leakage through the membrane domain boundary¹⁸ can explain the transient nature. The only other transient phenomenon that has been observed so far is the lipid extraction effect reported previously.⁴¹ That is why it was suggested that perhaps lipid extraction creates transient defects in membrane that cause ion leakage.⁴¹

3. Threshold of Daptomycin Concentration in the Membrane for Ion Leakage. Müller et al.¹⁸ suggested the delocalization of peripheral membrane proteins caused by daptomycin as the primary antibacterial mechanism, although they also detected depolarization of membrane potential that could also contribute to protein delocalization. Depolarization by itself could cause also cell death.¹ Here we discuss the implications of our results on ion leakage induced by daptomycin.

Comparison of the results presented in panels a and b of Figure 1 with those in panel c of Figure 1 implies that there was a threshold of daptomycin concentration in the membrane, below which daptomycin did not cause ion leakage. For example, in panels a and b of Figure 1, the membrane area increased to $\sim 3.5\%$ before the occurrence of ion leakage, implying a threshold of the bound daptomycin:lipid ratio of $\sim 1:100$ (see the ballpark estimate in the Supporting Information). A counter example of no concentration threshold is ionomycin. The initial response of GUVs to daptomycin is similar to the initial response to melittin;³⁰ compare Movie 1a and Movie 1b with Movie melittin. In the latter case, there is a more precisely measured melittin:lipid threshold of 1:45 before pore formation occurs,⁵⁶ and the melittin threshold has been correlated to the change in the orientation of the helical peptide from parallel to the membrane to perpendicular to the membrane.^{30,56} In comparison, it has been difficult to investigate the molecular state of daptomycin bound in the membrane. There is clear evidence of daptomycin oligomerization or clustering in the membrane provided by fluorescence resonance energy transfer (FRET).^{53,57,58} Co-clustering of daptomycin with PG was inferred from fluorescence imaging, which also showed that the clustering or daptomycin did not

transmit through the membrane.⁴⁴ There are hypotheses for the oligomerization sizes,^{19,53} but so far, these hypotheses are not based on experimental methods that are capable of measuring the sizes. The idea of daptomycin ion channels^{17,53–55} was also largely based on the detection of FRET, but it contradicts the experimental evidence presented by Müller et al.¹⁸ and that presented here.

Of particular significance is the combination of these two features, i.e., differential bindings to different fluidities of membrane and the existence of a concentration threshold of bound daptomycin for ion leakage. In the absence of a threshold, a weak binding can still achieve the effect of ion leakage as demonstrated by a very low concentration of ionomycin in Figure 3. In our prior study, we have shown that there is a minimum solution concentration of daptomycin below which GUV protrusion length would increase to a maximum level but would not decrease, indicating no ion leakage.⁴¹

Lastly, there is a suggestion by Taylor et al.⁵⁹ that two successive calcium-dependent transitions mediate membrane binding and oligomerization of daptomycin. This would be an attractive idea for explaining the concentration threshold or the transient nature of leakage if it were proven by experiment, and it was adopted in the working model by Müller et al.¹⁸ However, this “sequential two-site model”⁵⁹ was based on an isothermal titration calorimetry (ITC) measurement. ITC measures the heat of reaction. It is ideal for measuring, for example, the binding of the neutral peptide to bilayers, because in this case the heat of reaction per peptide is constant. For charged peptides, the heat of reaction would change with the degree of binding; therefore, the binding isotherm of charged peptides to membrane is model-dependent, i.e., with no definitive conclusion. This was explained in great detail by Seelig.⁶⁰ Daptomycin binding is even more complicated. It involves many types of possible bindings among daptomycin, Ca²⁺, and PG-containing lipid bilayers. Taylor et al.⁵⁹ performed a single titration of CaCl₂ into a suspension of daptomycin and lipid vesicles, and from model fitting, they concluded with the sequential two-site model. It is safe to say it is impossible to single out one model from many other possibilities on the basis of one heat of reaction measurement. We believe that the crucial missing information for understanding daptomycin can be obtained only by probing the structure and distribution of daptomycin in membranes.

■ ASSOCIATED CONTENT

Supporting Information

The Supporting Information is available free of charge on the ACS Publications website at DOI: 10.1021/acs.biochem.8b00818.

CD spectra of daptomycin in DOPE/DOPG and DOPC/DOPG vesicle suspensions (Figure S1), vesicle size as a function of Ca²⁺ concentration determined by DLS (Figure S2), control experiments for the micro-pipet-aspirated GUV experiment (Figure S3), kinetic deceleration of ionomycin-induced ion leakage at low ionomycin concentrations (Figure S4), daptomycin that permeabilizes only lipid bilayers containing PG (Figure S5), K⁺ sensitive electric potential that is proportional to the logarithm of the K⁺ concentration (Figure S6), a control experiment showing daptomycin produces a potassium ion potential in the absence of K⁺ (Figure

S7), and an estimate of the threshold concentration of bound daptomycin in the lipid bilayer (PDF)

Movie 1a for Figure 1a (AVI)

Movie 1b for Figure 1b (AVI)

Movie melittin for comparison (AVI)

■ AUTHOR INFORMATION

Corresponding Author

*E-mail: hwhuang@rice.edu.

ORCID

Meng-Hsuan Hsieh: 0000-0003-1414-5975

Huey W. Huang: 0000-0002-4107-0289

Funding

This work was supported by Taiwan MOST 105-2112-M-213-002 (to M.-T.L.), National Institutes of Health Grant GM55203 (to H.W.H.), and Robert A. Welch Foundation Grant C-0991 (to H.W.H.).

Notes

The authors declare no competing financial interest.

■ REFERENCES

- (1) Silverman, J. A., Perlmutter, N. G., and Shapiro, H. M. (2003) Correlation of daptomycin bactericidal activity and membrane depolarization in *Staphylococcus aureus*. *Antimicrob. Agents Chemother.* 47, 2538–2544.
- (2) Allen, N. E., Hobbs, J. N., and Alborn, W. E., Jr. (1987) Inhibition of peptidoglycan biosynthesis in gram-positive bacteria by LY146032. *Antimicrob. Agents Chemother.* 31, 1093–1099.
- (3) Cottagnoud, P. (2008) Daptomycin: a new treatment for insidious infections due to gram-positive pathogens. *Swiss Med. Wkly.* 138, 93–99.
- (4) Mascio, C. T., Alder, J. D., and Silverman, J. A. (2007) Bactericidal action of daptomycin against stationary-phase and nondividing *Staphylococcus aureus* cells. *Antimicrob. Agents Chemother.* 51, 4255–4260.
- (5) Hobbs, J. K., Miller, K., O'Neill, A. J., and Chopra, I. (2008) Consequences of daptomycin-mediated membrane damage in *Staphylococcus aureus*. *J. Antimicrob. Chemother.* 62, 1003–1008.
- (6) Pogliano, J., Pogliano, N., and Silverman, J. A. (2012) Daptomycin-mediated reorganization of membrane architecture causes mislocalization of essential cell division proteins. *J. Bacteriol.* 194, 4494–4504.
- (7) Cotroneo, N., Harris, R., Perlmutter, N., Beveridge, T., and Silverman, J. A. (2008) Daptomycin exerts bactericidal activity without lysis of *Staphylococcus aureus*. *Antimicrob. Agents Chemother.* 52, 2223–2225.
- (8) Arias, C. A., Panesso, D., McGrath, D. M., Qin, X., Mojica, M. F., Miller, C., Diaz, L., Tran, T. T., Rincon, S., Barbu, E. M., Reyes, J., Roh, J. H., Lobos, E., Sodergren, E., Pasqualini, R., Arap, W., Quinn, J. P., Shamoo, Y., Murray, B. E., and Weinstock, G. M. (2011) Genetic basis for in vivo daptomycin resistance in enterococci. *N. Engl. J. Med.* 365, 892–900.
- (9) Friedman, L., Alder, J. D., and Silverman, J. A. (2006) Genetic changes that correlate with reduced susceptibility to daptomycin in *Staphylococcus aureus*. *Antimicrob. Agents Chemother.* 50, 2137–2145.
- (10) Hachmann, A. B., Sevim, E., Gaballa, A., Popham, D. L., Antelmann, H., and Helmann, J. D. (2011) Reduction in membrane phosphatidylglycerol content leads to daptomycin resistance in *Bacillus subtilis*. *Antimicrob. Agents Chemother.* 55, 4326–4337.
- (11) Palmer, K. L., Daniel, A., Hardy, C., Silverman, J., and Gilmore, M. S. (2011) Genetic basis for daptomycin resistance in enterococci. *Antimicrob. Agents Chemother.* 55, 3345–3356.
- (12) Davlieva, M., Zhang, W., Arias, C. A., and Shamoo, Y. (2013) Biochemical characterization of cardiolipin synthase mutations associated with daptomycin resistance in enterococci. *Antimicrob. Agents Chemother.* 57, 289–296.

- (13) Jones, T., Yeaman, M. R., Sakoulas, G., Yang, S. J., Proctor, R. A., Sahl, H. G., Schrenzel, J., Xiong, Y. Q., and Bayer, A. S. (2008) Failures in clinical treatment of *Staphylococcus aureus* Infection with daptomycin are associated with alterations in surface charge, membrane phospholipid asymmetry, and drug binding. *Antimicrob. Agents Chemother.* 52, 269–278.
- (14) Hachmann, A. B., Angert, E. R., and Helmann, J. D. (2009) Genetic analysis of factors affecting susceptibility of *Bacillus subtilis* to daptomycin. *Antimicrob. Agents Chemother.* 53, 1598–1609.
- (15) Wale, L. J., Shelton, A. P., and Greenwood, D. (1989) Scanning electronmicroscopy of *Staphylococcus aureus* and *Enterococcus faecalis* exposed to daptomycin. *J. Med. Microbiol.* 30, 45–49.
- (16) Alborn, W. E., Jr., Allen, N. E., and Preston, D. A. (1991) Daptomycin disrupts membrane potential in growing *Staphylococcus aureus*. *Antimicrob. Agents Chemother.* 35, 2282–2287.
- (17) Zhang, T., Muraih, J. K., McCormick, B., Silverman, J., and Palmer, M. (2014) Daptomycin forms cation- and size-selective pores in model membranes. *Biochim. Biophys. Acta, Biomembr.* 1838, 2425–2430.
- (18) Muller, A., Wenzel, M., Strahl, H., Grein, F., Saaki, T. N., Kohl, B., Siersma, T., Bandow, J. E., Sahl, H. G., Schneider, T., and Hamoen, L. W. (2016) Daptomycin inhibits cell envelope synthesis by interfering with fluid membrane microdomains. *Proc. Natl. Acad. Sci. U. S. A.* 113, E7077–E7086.
- (19) Straus, S. K., and Hancock, R. E. (2006) Mode of action of the new antibiotic for Gram-positive pathogens daptomycin: comparison with cationic antimicrobial peptides and lipopeptides. *Biochim. Biophys. Acta, Biomembr.* 1758, 1215–1223.
- (20) Taylor, S. D., and Palmer, M. (2016) The action mechanism of daptomycin. *Bioorg. Med. Chem.* 24, 6253–6268.
- (21) Lenarcic, R., Halbedel, S., Visser, L., Shaw, M., Wu, L. J., Errington, J., Marenduzzo, D., and Hamoen, L. W. (2009) Localisation of DivIVA by targeting to negatively curved membranes. *EMBO J.* 28, 2272–2282.
- (22) Ramamurthi, K. S., and Losick, R. (2009) Negative membrane curvature as a cue for subcellular localization of a bacterial protein. *Proc. Natl. Acad. Sci. U. S. A.* 106, 13541–13545.
- (23) Taylor, R., Beriashvili, D., Taylor, S., and Palmer, M. (2017) Daptomycin Pore Formation Is Restricted by Lipid Acyl Chain Composition. *ACS Infect. Dis.* 3, 797–801.
- (24) Sun, Y., Lee, C. C., Hung, W. C., Chen, F. Y., Lee, M. T., and Huang, H. W. (2008) The bound states of amphiphatic drugs in lipid bilayers: study of curcumin. *Biophys. J.* 95, 2318–2324.
- (25) Angelova, M. I. (2000) Liposome Electroformation. In *Giant Vesicles* (Luisi, P. L., and Walde, P., Eds.) pp 27–36, John Wiley & Sons, Chichester, U.K.
- (26) Gee, K. R., Brown, K. A., Chen, W. N., Bishop-Stewart, J., Gray, D., and Johnson, I. (2000) Chemical and physiological characterization of fluo-4 Ca(2+)-indicator dyes. *Cell Calcium* 27, 97–106.
- (27) Joe, B., Vijaykumar, M., and Lokesh, B. R. (2004) Biological properties of curcumin-cellular and molecular mechanisms of action. *Crit. Rev. Food Sci. Nutr.* 44, 97–111.
- (28) Kuchnir Fygenon, D., Elbaum, M., Shraiman, B., and Libchaber, A. (1997) Microtubules and vesicles under controlled tension. *Phys. Rev. E: Stat. Phys., Plasmas, Fluids, Relat. Interdiscip. Top.* 55, 850–859.
- (29) Sun, Y., Hung, W. C., Chen, F. Y., Lee, C. C., and Huang, H. W. (2009) Interaction of tea catechin (–)-epigallocatechin gallate with lipid bilayers. *Biophys. J.* 96, 1026–1035.
- (30) Lee, M. T., Sun, T. L., Hung, W. C., and Huang, H. W. (2013) Process of inducing pores in membranes by melittin. *Proc. Natl. Acad. Sci. U. S. A.* 110, 14243–14248.
- (31) Kwok, R., and Evans, E. (1981) Thermoelasticity of large lecithin bilayer vesicles. *Biophys. J.* 35, 637–652.
- (32) Katsu, T., Imamura, T., Komagoe, K., Masuda, K., and Mizushima, T. (2007) Simultaneous measurements of K⁺ and calcein release from liposomes and the determination of pore size formed in a membrane. *Anal. Sci.* 23, 517–522.
- (33) Lee, M. T., Hung, W. C., Hsieh, M. H., Chen, H., Chang, Y. Y., and Huang, H. W. (2017) Molecular State of the Membrane-Active Antibiotic Daptomycin. *Biophys. J.* 113, 82–90.
- (34) Gidden, J., Denson, J., Liyanage, R., Ivey, D. M., and Lay, J. O. (2009) Lipid Compositions in *Escherichia coli* and *Bacillus subtilis* During Growth as Determined by MALDI-TOF and TOF/TOF Mass Spectrometry. *Int. J. Mass Spectrom.* 283, 178–184.
- (35) Lewis, R. N., Zhang, Y. P., and McElhaney, R. N. (2005) Calorimetric and spectroscopic studies of the phase behavior and organization of lipid bilayer model membranes composed of binary mixtures of dimyristoylphosphatidylcholine and dimyristoylphosphatidylglycerol. *Biochim. Biophys. Acta, Biomembr.* 1668, 203–214.
- (36) Jung, D., Powers, J. P., Straus, S. K., and Hancock, R. E. (2008) Lipid-specific binding of the calcium-dependent antibiotic daptomycin leads to changes in lipid polymorphism of model membranes. *Chem. Phys. Lipids* 154, 120–128.
- (37) Zhang, J., Scott, W. R. P., Gabel, F., Wu, M., Desmond, R., Bae, J., Zaccai, G., Algar, W. R., and Straus, S. K. (2017) On the quest for the elusive mechanism of action of daptomycin: Binding, fusion, and oligomerization. *Biochim. Biophys. Acta, Proteins Proteomics* 1865, 1490–1499.
- (38) Papahadjopoulos, D., Poste, G., Schaeffer, B. E., and Vail, W. J. (1974) Membrane fusion and molecular segregation in phospholipid vesicles. *Biochim. Biophys. Acta, Biomembr.* 352, 10–28.
- (39) Barry, A. L., Fuchs, P. C., and Brown, S. D. (2001) In vitro activities of daptomycin against 2,789 clinical isolates from 11 North American medical centers. *Antimicrob. Agents Chemother.* 45, 1919–1922.
- (40) Beeler, T. J., Jona, I., and Martonosi, A. (1979) The effect of ionomycin on calcium fluxes in sarcoplasmic reticulum vesicles and liposomes. *J. Biol. Chem.* 254, 6229–6231.
- (41) Chen, Y. F., Sun, T. L., Sun, Y., and Huang, H. W. (2014) Interaction of daptomycin with lipid bilayers: a lipid extracting effect. *Biochemistry* 53, 5384–5392.
- (42) Lee, C. C., Sun, Y., and Huang, H. W. (2010) Membrane-mediated peptide conformation change from alpha-monomers to beta-aggregates. *Biophys. J.* 98, 2236–2245.
- (43) Sun, Y., Lee, C. C., Chen, T. H., and Huang, H. W. (2010) Kinetic Process of beta-Amyloid Formation via Membrane Binding. *Biophys. J.* 99, 544–552.
- (44) Kreuzberger, M. A., Pokorny, A., and Almeida, P. F. (2017) Daptomycin-Phosphatidylglycerol Domains in Lipid Membranes. *Langmuir* 33, 13669–13679.
- (45) Seigneuret, M., and Devaux, P. F. (1984) ATP-dependent asymmetric distribution of spin-labeled phospholipids in the erythrocyte membrane: relation to shape changes. *Proc. Natl. Acad. Sci. U. S. A.* 81, 3751–3755.
- (46) Martin, O. C., and Pagano, R. E. (1987) Transbilayer movement of fluorescent analogs of phosphatidylserine and phosphatidylethanolamine at the plasma membrane of cultured cells. Evidence for a protein-mediated and ATP-dependent process(es). *J. Biol. Chem.* 262, 5890–5898.
- (47) Rodriguez, N., Heuvingh, J., Pincet, F., and Cribier, S. (2005) Indirect evidence of submicroscopic pores in giant unilamellar [correction of unilamellar] vesicles. *Biochim. Biophys. Acta, Gen. Subj.* 1724, 281–287.
- (48) Hung, W. C., Lee, M. T., Chen, F. Y., and Huang, H. W. (2007) The condensing effect of cholesterol in lipid bilayers. *Biophys. J.* 92, 3960–3967.
- (49) Needham, D., and Nunn, R. S. (1990) Elastic deformation and failure of lipid bilayer membranes containing cholesterol. *Biophys. J.* 58, 997–1009.
- (50) Hkadyk, S. B., and Haydon, D. A. (1984) Ion Movements in Gramicidin Channels. In *Current Topics in Membranes and Transport* (Stein, W. D., Ed.) pp 327–372, Academic Press, New York.
- (51) Mayers, D. F., and Urry, D. W. (1972) Valinomycin-cation complex. Conformational energy aspects. *J. Am. Chem. Soc.* 94, 77–81.

(52) Sun, Y., Hung, W. C., Lee, M. T., and Huang, H. W. (2015) Membrane-mediated amyloid formation of PrP 106–126: A kinetic study. *Biochim. Biophys. Acta, Biomembr.* 1848, 2422–2429.

(53) Muraih, J. K., and Palmer, M. (2012) Estimation of the subunit stoichiometry of the membrane-associated daptomycin oligomer by FRET. *Biochim. Biophys. Acta, Biomembr.* 1818, 1642–1647.

(54) Zhang, T., Muraih, J. K., Mintzer, E., Tishbi, N., Desert, C., Silverman, J., Taylor, S., and Palmer, M. (2013) Mutual inhibition through hybrid oligomer formation of daptomycin and the semi-synthetic lipopeptide antibiotic CB-182,462. *Biochim. Biophys. Acta, Biomembr.* 1828, 302–308.

(55) Zhang, T., Muraih, J. K., Tishbi, N., Herskowitz, J., Victor, R. L., Silverman, J., Uwumarenogie, S., Taylor, S. D., Palmer, M., and Mintzer, E. (2014) Cardiolipin prevents membrane translocation and permeabilization by daptomycin. *J. Biol. Chem.* 289, 11584–11591.

(56) Yang, L., Harroun, T. A., Weiss, T. M., Ding, L., and Huang, H. W. (2001) Barrel-stave model or toroidal model? a case study on melittin pores. *Biophys. J.* 81, 1475–1485.

(57) Muraih, J. K., Pearson, A., Silverman, J., and Palmer, M. (2011) Oligomerization of daptomycin on membranes. *Biochim. Biophys. Acta, Biomembr.* 1808, 1154–1160.

(58) Muraih, J. K., Harris, J., Taylor, S. D., and Palmer, M. (2012) Characterization of daptomycin oligomerization with perylene excimer fluorescence: stoichiometric binding of phosphatidylglycerol triggers oligomer formation. *Biochim. Biophys. Acta, Biomembr.* 1818, 673–678.

(59) Taylor, R., Butt, K., Scott, B., Zhang, T., Muraih, J. K., Mintzer, E., Taylor, S., and Palmer, M. (2016) Two successive calcium-dependent transitions mediate membrane binding and oligomerization of daptomycin and the related antibiotic AS4145. *Biochim. Biophys. Acta, Biomembr.* 1858, 1999–2005.

(60) Seelig, J. (1997) Titration calorimetry of lipid-peptide interactions. *Biochim. Biophys. Acta, Rev. Biomembr.* 1331, 103–116.

Supplemental Information

for

Comparison of the Effects of Daptomycin on Bacterial and Model Membranes

Ming-Tao Lee^{1,2}, Pei-Yin Yang³, Nicholas E. Charron³, Meng-Hsuan Hsieh⁴, Yu-Yung Chang¹, Huey W. Huang^{3*}

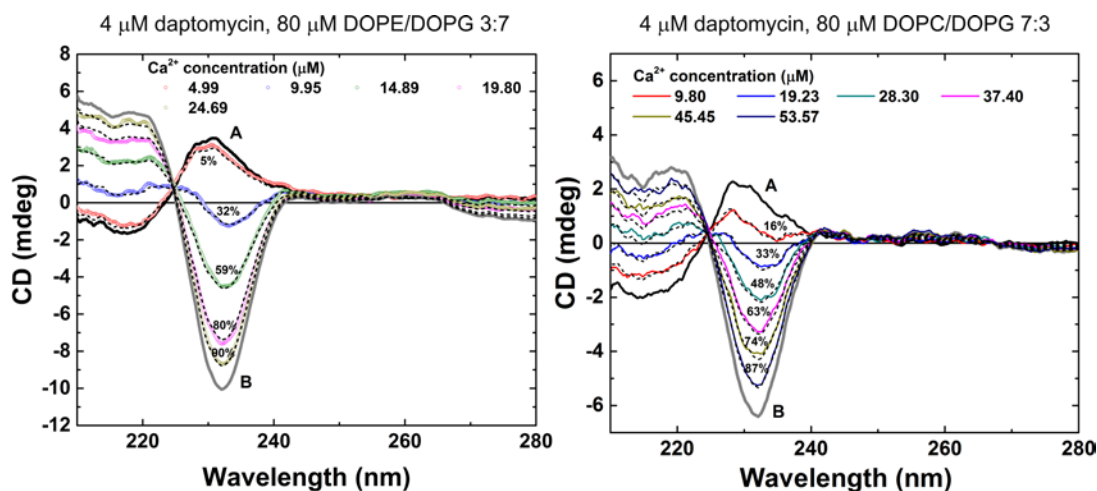
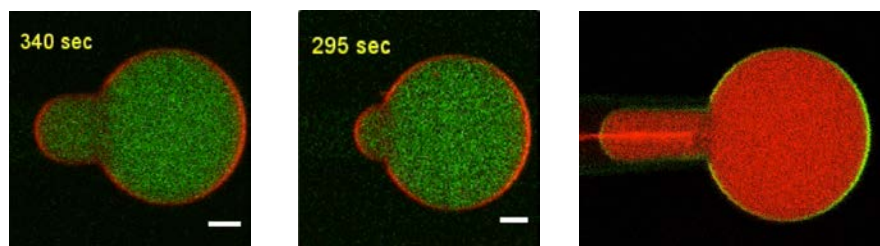


Fig. S1. Left, CD spectra of daptomycin in a suspension of DOPE/DOPG 3:7 vesicles with various Ca²⁺ concentrations. Right, CD spectra of daptomycin in a suspension of DOPC/DOPG 7:3 vesicles reproduced from ¹ for comparison. In both cases, there are only two basis spectra: the A spectrum with no Ca²⁺, and the B spectrum at the highest Ca²⁺ concentration indicated in the box. At any other condition, the spectrum is a linear combination of A and B.

MOVIES for Fig. 1a, 1b and melittin (reproduced from ref ²)



Movie 1a: DOPE/DOPG 3:7 GUV, 0.3 μM daptomycin

Movie 1b: DOPC/DOPG 7:3 GUV, 1 μM daptomycin

Movie melittin: DOPC/DOPG 7:3 GUV, 2 μM FITC-melittin (from ref. ²)

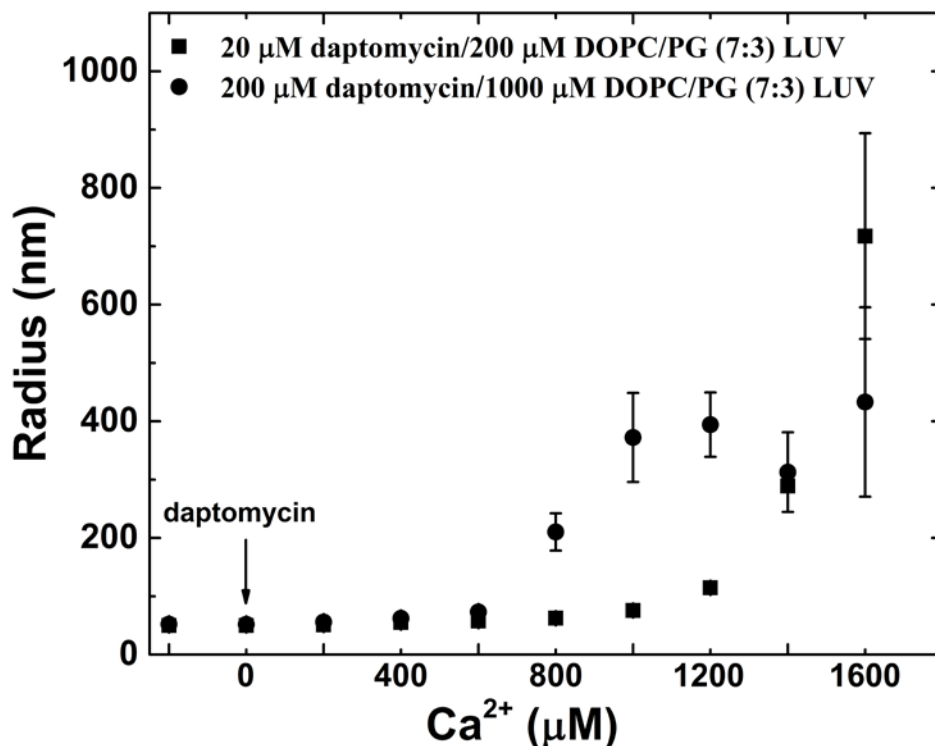


Fig. S2 Average radius of DOPC/DOPG 7:3 vesicles measured by dynamic light scattering. (LUVs were produced by extruding through polycarbonate filters of pore size 100 nm.) Each condition was allowed to equilibrate for 20 mins under constant stirring. (1) For Ca²⁺ leak-in experiments, the concentrations of daptomycin were less than 20 μM and the highest lipid concentration was 200 μM. There is no aggregation or fusion of vesicles at or below Ca²⁺ concentration 1 mM. (2) For K⁺ leak-out experiment, the highest concentration of daptomycin was 200 μM, lipid 1000 μM. There is no aggregation or fusion of vesicles at or below Ca²⁺ concentration 500 μM. The mean and the standard deviation of the mean are obtained from multiple measurements.

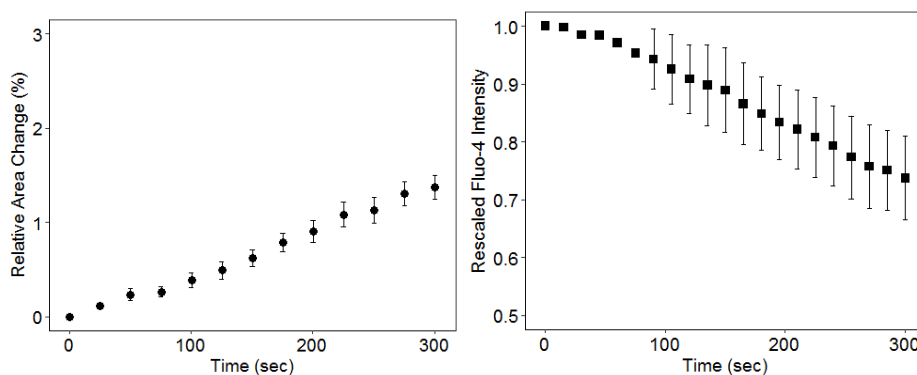


Fig. S3. Control experiments. (Left) Background membrane area change due to water evaporation from the observation chamber, as calculated by the GUV protrusion length increase (see Method). GUVs were made of DOPE/DOPG 3:7. The same control experiments were performed for DOPC/DOPG 7:3 in ref³. Both inside and outside of the GUV contained the same control solution. Control experiments were also performed by including either daptomycin or calcium ions in the chamber, but not both. The results were similar. (Right) Photobleaching of calcium activated Fluo-4 fluorescence intensity. GUVs encapsulated 199 mM sucrose, 1 mM Tris-HCl (pH 7.0), 40 μ M Fluo-4 and 20 μ M CaCl_2 . The chamber solution was 190 mM glucose and 10 mM Tris-HCl (pH=7.4). The mean and the standard deviation of the mean are obtained from multiple measurements.

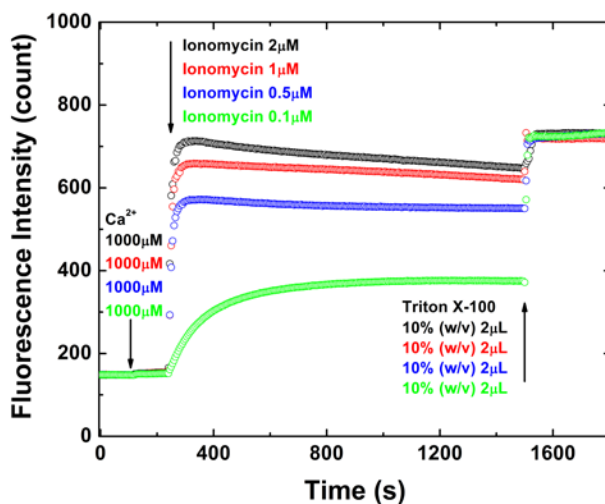


Fig. S4 Kinetic slow-down (decreasing slope of increase) of ion leakage by ionomycin at very low concentrations ($\approx 0.1 \mu\text{M}$) is consistent with ionomycin being an ion carrier embedded in the membrane. The ion transport by ion carriers involves diffusion of the carriers inside the membrane.

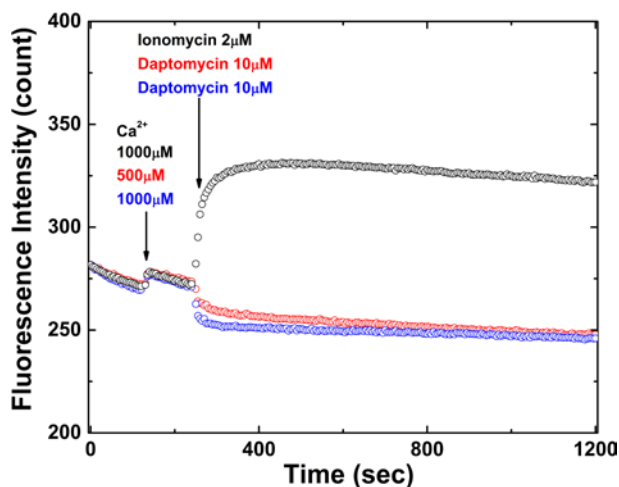


Fig. S5 Daptomycin permeabilizes only lipid bilayers containing PG. Here the samples were LUVs of DOPC encapsulated 10 μM Fluo-4. These samples had residual Fluo-4 in the outside solution. When Ca^{2+} was added (before ionomycin or daptomycin), the fluorescence intensity increased slightly due to the residual Fluo-4 outside the LUVs. The addition of ionomycin caused Ca^{2+} leak-in to the LUVs, same as in Fig. 2a where DOPC/DOPG was used. However, the addition of daptomycin did not cause ion leak-in to the DOPC vesicles, in contrast to Fig. 2b where DOPC/DOPG was used. Daptomycin has a higher binding affinity to Ca^{2+} than does Fluo-4, hence the fluorescence intensity of Fluo-4 outside the vesicles decreased when daptomycin was added. It appears that the calcium bound to Fluo-4 was taken by daptomycin.

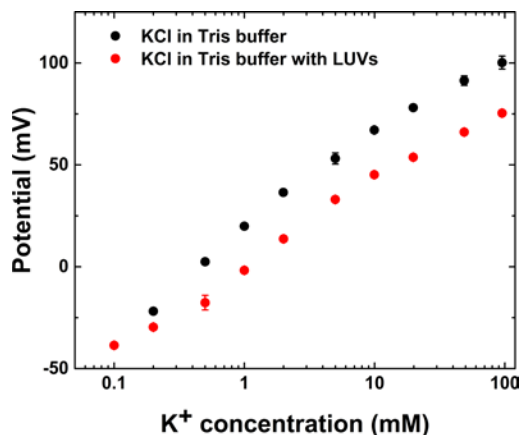


Fig. S6 Electric potential is proportional to the logarithm of K^+ concentration. Black: KCl in 10 mM Tris buffer. Red: KCl in 10 mM Tris buffer and 0.5 mM DOPC/DOPG 7:3 LUV.

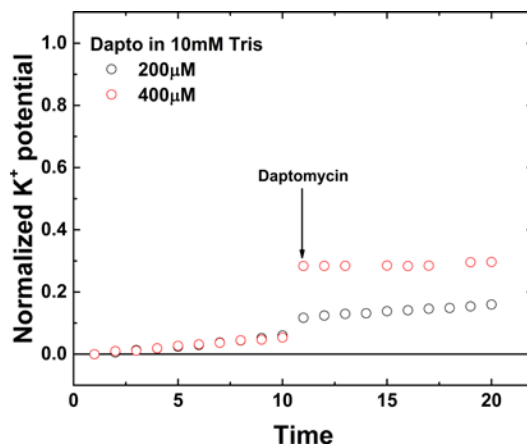


Fig. S7 Daptomycin produces a potassium ion potential in the absence of K⁺. This is treated as a background to be removed. The data in Fig 4a are after this background subtraction.

Estimate of the threshold concentration of bound daptomycin in lipid bilayer

- 1) Assuming the radius of GUV is 25 μm , its membrane area is $78 \times 10^{10} \text{ \AA}^2$ which contains about 1.3×10^{10} lipid molecules in each leaflet of the bilayer.
- 2) 3.5% increase of the membrane area is $2.7 \times 10^{10} \text{ \AA}^2$.
- 3) Daptomycin MW is 1620, its molecular volume is $\sim 2700 \text{ \AA}^3$, molecular area $\sim 200 \text{ \AA}^2$.
- 4) Assuming that the membrane area increase is due to the inclusion of daptomycin. Then there are 1.4×10^8 daptomycin molecules in each leaflet of the bilayer.
- 5) Thus the bound daptomycin to lipid ratio is $1.4 \times 10^8 / 1.3 \times 10^{10} \sim 1/100$. This estimate could be wrong by a factor as much as ~ 2 , because the molecular area of an inserted daptomycin is difficult to estimate (see ref. ⁴).

Supplemental References

- [1] Lee, M. T., Hung, W. C., Hsieh, M. H., Chen, H., Chang, Y. Y., and Huang, H. W. (2017) Molecular State of the Membrane-Active Antibiotic Daptomycin, *Biophys J* 113, 82-90.
- [2] Lee, M. T., Sun, T. L., Hung, W. C., and Huang, H. W. (2013) Process of inducing pores in membranes by melittin, *Proc Natl Acad Sci U S A* 110, 14243-14248.
- [3] Chen, Y. F., Sun, T. L., Sun, Y., and Huang, H. W. (2014) Interaction of daptomycin with lipid bilayers: a lipid extracting effect, *Biochemistry* 53, 5384-5392.
- [4] Lee, M. T., Hung, W. C., Chen, F. Y., and Huang, H. W. (2005) Many-body effect of antimicrobial peptides: on the correlation between lipid's spontaneous curvature and pore formation, *Biophys J* 89, 4006-4016.